

# An Adaptive Robotics Framework for Chemistry Lab Automation

Naruki Yoshikawa<sup>\*1</sup>, Andrew Zou Li<sup>\*1</sup>, Kourosh Darvish<sup>\*†1</sup>, Yuchi Zhao<sup>\*2</sup>, Haoping Xu<sup>\*1</sup>,  
 Alán Aspuru-Guzik<sup>1</sup>, Animesh Garg<sup>1,3</sup>, Florian Shkurti<sup>1</sup>

**Abstract**—In the process of materials discovery, chemists currently need to perform many laborious, time-consuming, and often dangerous lab experiments. To accelerate this process, we propose a framework for robots to assist chemists by performing lab experiments autonomously. The solution allows a general-purpose robot to perform diverse chemistry experiments and efficiently make use of available lab tools. Our system can load high-level descriptions of chemistry experiments, perceive a dynamic workspace, and autonomously plan the required actions and motions to perform the given chemistry experiments with common tools found in the existing lab environment. Our architecture uses a modified PDDLStream solver for integrated task and constrained motion planning, which generates plans and motions that are guaranteed to be safe by preventing collisions and spillage. We present a modular framework that can scale to many different experiments, actions, and lab tools. In this work, we demonstrate the utility of our framework on three pouring skills and two foundational chemical experiments for materials synthesis: solubility and recrystallization. More experiments and updated evaluations can be found at <https://ac-rad.github.io/arc-icra2023>.

## I. INTRODUCTION

Chemistry experiments are essential for finding new materials or verifying hypotheses in materials science. These experiments are typically conducted by human chemists, but they are laborious, time-consuming, and often dangerous. This work aims to enable general-purpose robot manipulators to perform chemistry experiments, thus reducing the work of chemists and accelerating new findings in science. Further, robots can potentially reduce risks in experiments involving dangerous (radioactive or carcinogenic) materials.

We propose a flexible and modular robotic framework that uses a general-purpose collaborative robot arm to autonomously execute experiments in a semi-structured chemistry lab, given only a high-level description of the desired experiment and a PDDLStream [1] problem description. Our framework is general enough to find plans informed by visual perception and execute multiple chemistry experiments.

One of the difficulties in automating chemical experiments is the cost of introducing specialized hardware, specifically designed to conduct a single experiment and often immutable and not programmable. This strategy cannot be scaled, since the range of chemical experiments is diverse and requires adaptation. Moreover, current chemistry equipment is designed for human use and laboratory environments are semi-structured. Hence, any robotic solution for lab automation is required to operate in semi-structured environments and use



Fig. 1: Robot pouring granular material during an experiment.

tools designed for humans.

The deployment of robots in chemistry laboratories poses many challenges. First, robots should recognize objects in the chemistry lab, such as transparent glassware, opaque tools, objects, or substances; segment and recognize the contents of vessels; and estimate object poses [2]. Robots should perceive and monitor the state of the materials synthesis experiment; for example, in a chemical solution, the robot should know when the solute is fully dissolved inside the solvent [3]. Second, robots should be able to perform dexterous manipulation of objects to perform a large repertoire of tasks. Some examples are constrained motion generation for picking and transporting objects such as beakers while avoiding spillage; pouring skills; manipulation of tools; handling rigid, deformable, and granular objects; and transporting glassware filled with liquids and powders. Third, robots should map high-level experiment descriptions to robot actions while accounting for safety considerations.

Among the challenges described above, our paper primarily focuses on the second category related to task and motion planning and the manipulation of glassware in pouring tasks.

We present three major contributions: *i*) a scalable framework for chemistry lab automation that enables a robot to safely execute long-horizon chemistry experiments that involve liquids, powders, and solids in the chemistry lab; *ii*) providing guarantees for constrained motion planning in PDDLStream, which is required for avoiding spillage while transporting liquids and other materials. We do this with a 37.5% increase in the minimum planning time compared to unconstrained motion planning; *iii*) a set of accurate and efficient pouring skills inspired by human behavior, with an average error of 2g and pouring times of less than 10s

<sup>\*</sup> Authors contributed equally, <sup>1</sup>University of Toronto & Vector Institute, <sup>2</sup>University of Waterloo, <sup>3</sup>Nvidia, <sup>†</sup>Corresponding author.

over 15 trials. We validate the utility of our framework by conducting two chemistry experiments: measurement of *solubility* and *recrystallization*. We attained 3.42% error for the solubility of salt and successfully recrystallized alum—two fundamental types of chemistry experiments.

## II. RELATED WORK

**Lab Automation** – An example of lab automation is the Robot Scientist Adam [4], [5], who automated hypothesis generation and experimental selection to determine a function of a yeast gene independently of human scientists. Another example is the usage of mobile robots for improving photocatalysts for hydrogen production from water [6].

Recently, an automated workflow that translates organic chemistry literature into a structured language called XDL was proposed [7]. ARChemist [8], a lab automation system, was developed to conduct experiments including solubility screening and crystallization without human intervention based on XDL descriptions.

Critically, none of the robot-assisted lab automation systems consider key task constraints, such as fixed end-effector orientation during the transfer of vessels filled with a liquid to prevent chemical spills or preemptively removing obstacles from the grasp region. Prior frameworks were tested in hand-tuned environments to avoid occurrences of unsatisfied task constraints. Further, existing setups do not incorporate perception to create the scene description, meaning that experiment setups must occur in static, structured environments. This dependency on predefined task and motion plans without constraint satisfaction guarantees limit the adaptability and robustness of prior frameworks upon scaling to new, dynamic workspaces. Our proposed framework resolves these gaps through constraint satisfaction guarantees and scene-aware planning with perception.

**Task and Motion Planning** – Task and motion planning (TAMP) simultaneously determines the sequence of high-level symbolic actions, such as picking and placing, and low-level motions for the action, such as trajectory generation. Several approaches have been proposed for the TAMP problem. Early approaches such as aSyMov [9] and SMAP [10] interleaved symbolic planners and motion planners. A similar approach was adopted in [11] for collaborative scenarios with the ability to make online decisions. FFRob [12] leveraged symbolic planners by creating symbolic actions from a sample of continuous motions. Monte Carlo tree search also has been applied to TAMP problems [13].

Another TAMP approach proposed in [1] is PDDLStream. It extends PDDL [14], a common language to describe a planning problem mainly targeting discrete actions and states, to continuous variables. PDDLStream reduces a continuous problem to a finite PDDL problem and invoke a classical PDDL solver as a subroutine. Recently, learning-based search heuristics for PDDLStream have been proposed to enhance its efficiency [15]. Nonetheless, PDDLStream does not yet account for task constraints in the planning process, which impedes its deployment to real-world lab environments. To overcome this shortcoming, our work *extends*

PDDLStream with constrained motion planning techniques to guarantee constraint satisfaction. A detailed review on TAMP approaches can be found in [16].

**Skills and Integration of Chemistry Lab Tools** – In the process of lab automation, robots interact with tools and objects within the workspace and require a repertoire of many laboratory skills. Some skills can be completed with existing instruments and sensors in chemistry labs, such as scales, stir plates, pH sensors, and heating instruments. Other skills are currently done either manually by humans in the lab or by expensive special instruments.

When the robot performs a skill, it may require different sensory inputs to compute the appropriate joint commands. For example, recent work using vision and weight feedback with methods based on PID control, intention learning, and understanding pouring dynamics have demonstrated that manipulators are capable of achieving milliliter accuracy in water pouring tasks with a variety of vessels at human-like speeds [17], [18]. In this work, we have reached similar results for pouring skills by using conventional scales. Another important skill in lab automation is constraint adherence [19], [20], as it is relevant to safety considerations and successful experiment execution, which we integrate into our TAMP module.

## III. METHODS

**Framework Overview** – Our proposed framework is composed of three components: *perception*, *task and motion planner* (TAMP), and *skill* module, shown in Fig. 2. A Chemical Description Language (XDL) [7] provides the experiment instructions as an input to the TAMP. The perception module updates the scene description by detecting the objects and estimating their positions using fiducial markers [21]. Currently, we assume prior knowledge of vessel contents and sizes, and each vessel is mapped to a unique marker ID. Given the instructions from XDL and the instantiated workspace state information from perception, an action sequence and robot trajectory are simultaneously generated by the TAMP module using PDDLStream. The resultant plan is then realized by the skill module and robot controller with perception feedback.

### A. Task and Motion Planning from XDL

The TAMP module converts experiment instructions given by XDL into PDDLStream goals and generates a motion plan. The TAMP algorithm is shown in Alg. 1.

**PDDLStream** – A PDDLStream problem described by a tuple  $(\mathcal{P}, \mathcal{A}, \mathcal{S}, \mathcal{O}, \mathcal{I}, \mathcal{G})$  is defined by a set of predicates  $\mathcal{P}$ , actions  $\mathcal{A}$ , streams  $\mathcal{S}$ , initial objects  $\mathcal{O}$ , an initial state  $\mathcal{I}$ , and a goal state  $\mathcal{G}$ . A predicate is a boolean function that describes the logical relationship of objects. An action  $a \in \mathcal{A}$  has a set of preconditions and effects. The action  $a$  can be executed when all the preconditions are satisfied, and the current state changes according to the effects after execution. The goal of PDDLStream planning is to find a sequence of actions starting from the initial state until all goals are satisfied, ensuring that the returned plan is valid

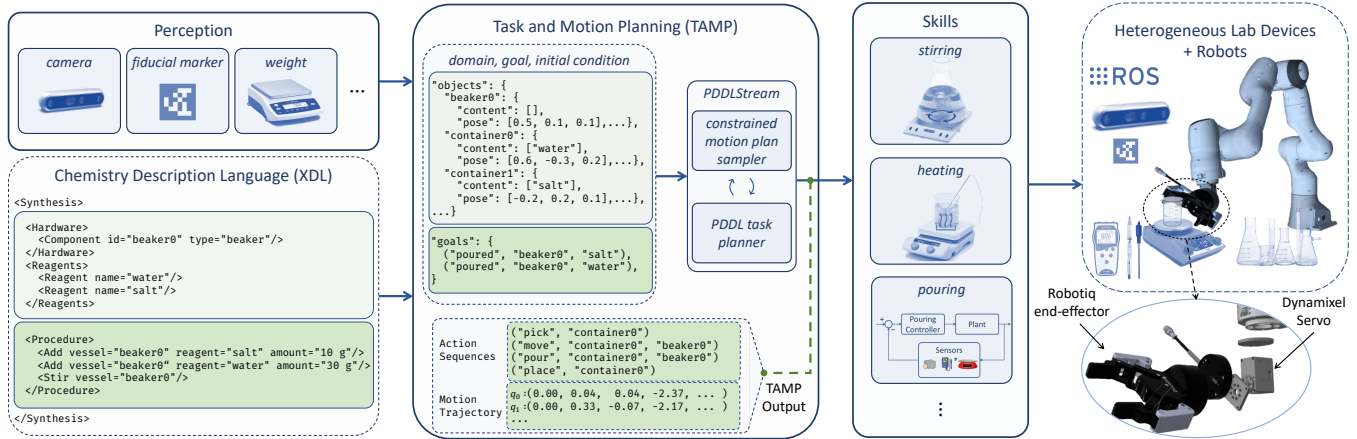


Fig. 2: **Framework for robot-assisted chemical synthesis:** composed of three *Perception*, *Task & Motion Planning*, and *Skills* blocks. The proposed framework enables the robot to leverage available chemistry lab devices (including sensors and actuators), by adding them to the robot network through ROS. The robot is equipped with an additional DOF at the end-effector, allowing it to perform constrained motions. The framework receives the chemical synthesis goal in XDL format. The *procedure* component is converted into corresponding PDDL goals, and *hardware* and *reagents* components identify the required initial condition for synthesis. *Perception* detects objects and estimates their positions and contents in the workspace. After, PDDLStream generates a sequence of actions to be executed by the robot.

and executable by the robot. We define four types of actions in our PDDLStream domain, including *pick*, *move*, *place*, and *pour*. For example, the *move* action translates the robot end-effector from a grasping pose to a placing or pouring pose using constrained motion planning. PDDLStream handles continuous motion using streams. Streams generate objects from continuous variables that satisfy specified conditions, such as feasible grasping pose and collision-free motion. An instance of a stream has a set of certified predicates that expands  $\mathcal{I}$  and functions as preconditions for other actions.

A PDDLStream problem is solved by leveraging a classical PDDL planner [22] with optimistic instantiation of streams (line 7). If a plan for the PDDL problem is found, the optimistic stream instances  $s \in \mathcal{S}$  in the plan are evaluated to determine the actual feasibility (line 8). If no plan was found or the streams are not feasible, other plans are explored with a larger set of optimistic stream instances.

**Chemical Description Language (XDL)** – XDL is a chemical programming language that describes chemical experiments in a standard format. It is based on XML syntax and is mainly composed of three mandatory sections: *Hardware*, *Reagents*, and *Procedure*. XDL instructions are parsed and passed to the TAMP module. The *Hardware* and *Reagents* sections are parsed as initial objects  $\mathcal{O}$ . *Procedure* is translated into a set of goals *Goals* (line 1).  $\mathcal{I}$  is generated from  $\mathcal{O}$  and sensory inputs (line 2). Each intermediate goal  $\mathcal{G} \in \text{Goals}$  is processed by PDDLStream (line 5). If a plan to attain  $\mathcal{G}$  is found, it is stored (line 10) and  $\mathcal{I}$  is updated according to the plan (line 11). After a set of plans to attain all goals is found, we obtain a complete motion plan (line 12).

### B. Constrained Motion Planning

To ensure that chemicals are not spilled during the manipulation of vessels, constrained motion planning is used to impose hard constraints on the end-effector orientation.

**Planning in a Constrained State Space** – Given a constraint on the geometry of the robot that lowers the dimensionality,

such as an end-effector orientation constraint, the planning problem resides on a constraint manifold  $\mathcal{M}$  embedded inside the original configuration space  $\mathcal{Q}$ . For some function of the joint state  $\mathbf{F}(q) : \mathcal{Q} \rightarrow \mathbb{R}^k$  derived from the  $k$  specified constraints, the constraint satisfaction condition is defined by the equality  $\mathbf{F}(q) = \mathbf{0}$ . Then, the constrained configuration space can be represented by the implicit manifold  $\mathcal{M} = \{q \in \mathcal{Q} \mid \mathbf{F}(q) = \mathbf{0}\}$ . The implicit nature of the manifold prevents planners from directly sampling, since the distribution of valid states is unknown. Further, since a manifold resides in a lower dimension than the configuration space, sampling valid states in the configuration space is highly improbable and thus impractical. Following the constrained motion planning framework developed in [23], our system integrates the projection-based method for finding constraint-satisfying configurations into the TAMP module as part of multiple streams. Using traditional sampling-based motion planning methods, we use a projection operator  $P : \mathcal{Q} \rightarrow \mathcal{M}$  to map sampled configurations in  $\mathcal{Q}$  to valid configurations in  $\mathcal{M}$  while preserving asymptotically optimal guarantees. We use probabilistic roadmap methods (PRM\*) to plan efficiently in the 8-DoF configuration space found in our chemistry laboratory domain. PRM\* is a multi-query planner that constructs a persistent probabilistic roadmap of  $\mathcal{Q}_{free}$  in a separate thread, allowing for multiple motion planning

### Algorithm 1 TAMPFORLABAUTOMATION()

**Input:** A XDL recipe  $\chi$ , sensory input  $\mathcal{H}$ , PDDLStream domain  $\mathcal{D}$

**Output:** Reference *plan* to execute

```

1:  $\text{Goals}, \mathcal{O} \leftarrow \text{XDLParser}(\chi)$  ▷ Objects
2:  $\mathcal{I} \leftarrow \text{PERCEPTION}(\mathcal{H}, \mathcal{O})$  ▷ Initial conditions
3: if not  $\text{PASSCONDITIONS}(\mathcal{I}, \mathcal{O})$  then return
4:  $\text{plan} = \emptyset, \mathcal{P} = \emptyset$ 
5: for all  $\mathcal{G} \in \text{Goals}$  do
6:   while  $\text{time}() \leq t_{max}$  do
7:      $\mathcal{P} = \text{OPTIMISTICPDDLSTREAMPLAN}(\mathcal{I}, \mathcal{G}, \mathcal{D})$ 
8:     if  $\mathcal{P} \neq \emptyset$  and  $\text{ISSTREAMFEASIBLE}(\mathcal{P})$  then break
9:   if  $\mathcal{P} = \emptyset$  then return
10:   $\text{plan} \leftarrow \text{plan} \cup \mathcal{P}$ 
11:   $\mathcal{I} = \text{UPDATESCENEREPRESENTATION}(\mathcal{I}, \mathcal{P})$ 
12: return plan
```

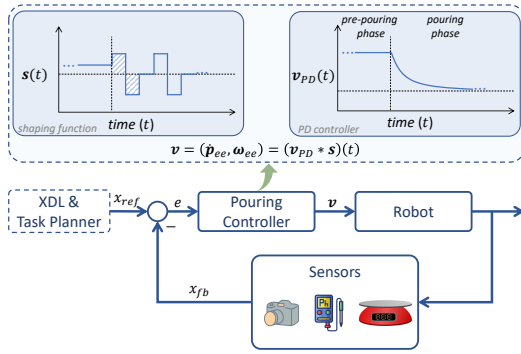


Fig. 3: **Pouring skill policy**: given the XDL & TAMP reference values and sensor feedback, the pouring controller computes the end-effector velocity for the robot using the convolution of a shaping function  $s(t)$  and a PD control output  $v_{PD}(t)$ .

queries to be solved without re-exploring the environment. **Inverse Kinematics for Constrained Motion Planning** – The constrained path planning problem is sensitive to the start and end states of the requested path, since paths between joint states may not be possible under strict or multiple constraints. If constrained planning is executed with any arbitrary valid solution from the IK solver, the planner typically fails. To address this shortcoming, two considerations are made. First, a multi-threaded IK solver with both iterative and random-based techniques is executed, and the solution that minimizes an objective function  $\phi$  is returned [24]. During grasping and placing, precision is paramount, and we only seek to minimize the sum-of-squares error between the start and goal Cartesian poses. Second, depending on the robot task, the objective function is extended to maximize the manipulability ellipsoid,  $\phi = \max \sqrt{\det(JJ^T)}$ , as described in [25]. This is applied for more complicated maneuvers, such as transferring liquids across the workspace. Finally, note that configuration sampling must account for the fact that multiple goal poses are possible; for example, any end-effector yaw angle is valid during parallel grasping but roll and pitch angles should be zero.

### C. Low-Level Skills for Task Planning

Chemistry lab skills require a particular suite of sensors, algorithms, and hardware. We provide an interface for instantiating different skill instances through ROS and simultaneously commanding them. For instance, recrystallization requires both pouring, heating, and stirring, which requires both weight feedback for volume estimation and skills for interacting with the liquid using available hardware.

In chemistry labs, a frequently used skill for synthesizing new materials is pouring. Pouring holds high intra-class variations depending on objectives (e.g., to reach a specific weight or pH value), substances (e.g., granulated solids or liquids), glassware (e.g., beaker, shaker, or squeeze bottle), and required precision. Pouring is a closed-loop process, in which feedback should be continuously monitored. Among these pouring actions, this work considers the following variations: pouring of liquid, pouring of granular solid and powders, and operating squeeze bottles. Note that, in contrast to many control problems, pouring is a non-reversible

process as we cannot compensate for overshoot.

Inspired by observations of chemists pouring reagents, we propose an algorithm that allows the robot to perform different pouring actions. As shown in Fig. 3, the proposed algorithm takes sensor measurements (e.g., weight feedback from the scale) as feedback and XDL experiment instructions for the reference pouring target. The algorithm outputs the robot end-effector joint velocity describing oscillations of the arm’s wrist. Since sensors are characterized by measurement delay, chemical reactions require time to stabilize, and pouring is a non-reversible action, chemists tend to pour a small amount of content from the pouring vessel into the target vessel. They periodically wait for some time and then pour again. In our approach, we use a shaping function  $s(t)$  to guide the direction and frequency of this oscillatory pouring behavior, while a PD controller lowers the pouring error. The end-effector velocity vector is computed by convoluting the shaping function  $s(t)$  over the PD control signal,  $v(t) = k_p e + k_d \dot{e}$ , where  $e(t) = x_{ref} - x_{fb}$ .

## IV. EXPERIMENTS AND EVALUATION

We evaluate the proposed framework with two component studies on pouring and constrained TAMP, and two types of experiments, solubility and recrystallization.

### A. Experiment Setup

The proposed lab automation framework has been evaluated using the Franka Emika Panda arm robot, equipped with a Robotiq 2F-85 gripper and an Intel RealSense D435i stereo camera mounted on the gripper to allow for active vision. The robot’s DoF has been extended by one degree (in total 8 DoF) at its end-effector using a Dynamixel XM540-W150 servo motor. The hardware setup is shown in Fig. 2. The robot is controlled using FrankaPy [26], and a ROS wrapper has been implemented for the servo motor. To detect fiducial markers, the AprilTag library is used [21]. We use the Open Motion Planning Library (OMPL) [27] and the MoveIt motion planning framework [28] for our TAMP module. OMPL’s constrained planning function [23] is used through a wrapper package which we extended from elion [29]. Visual information is gathered at the beginning of an experiment to construct a simulated environment representation for motion planning and visualization in RViz [30]. The framework is developed in C++/Python under ROS Melodic [31] on a Ubuntu 18.04 LTS 64-bit operating system. The workstation has an Intel Core i7-10700K 3.80 GHz  $\times$  16 thread CPU and 15.6 GiB of RAM. The framework was first tested in simulation using IsaacSim [32], which provided a virtual execution controller for the robot manipulator as well as virtual beakers and liquids.

**Robot Extension to 7+1 DoFs** – As shown in Fig. 2, the robot hardware is extended by one DoF for two purposes: *i*) to have a higher success rate for constrained motion planning, during which the effective degrees of freedom are reduced, and *ii*) to allow for parallel grasping (grripper parallel to the ground), which keeps the vessel opening unobstructed.

**Lab Tools Integration** – The robot can incorporate available lab tools to extend its abilities for performing chemical exper-



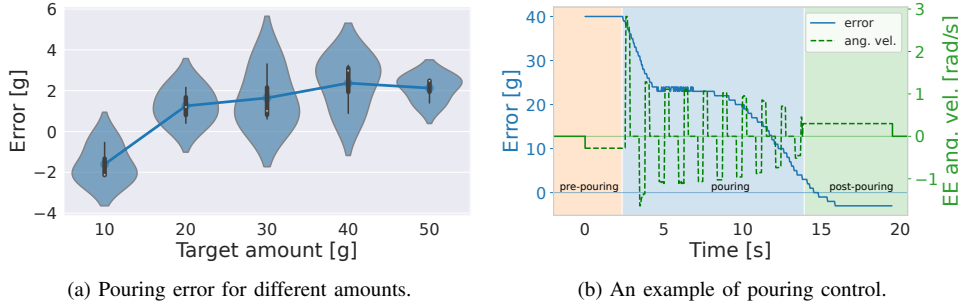


Fig. 4: **Evaluation of water pouring.** (a) The distribution of pouring error is shown on the violin plot. Experiments are repeated three times for each target amount. (b) This figure shows both the pouring error and the reference angular velocity of the robot end-effector when a 40 g target weight is requested.

iments, as indicated in Fig. 2. To perform the solubility and recrystallization experiments, we use an IKA RET control-visc device, commonly found in chemistry labs, to extend the robot skill set. This device works as a scale, hotplate, and stirplate. The scale precision is 1g with approximately  $\approx 3$  s of measurement delay. The device functionalities are exposed through the common skill interface and commutation from the robot to the device is instantiated via a RS-232 Serial to USB adapter.

### B. Component Evaluation

**Pouring** – The pouring skill evaluation is shown in Fig. 4. The accuracy of pouring (Fig. 4a) is measured by the final error. The average absolute error is  $2 \pm 1$  g for different pouring targets (mainly due to the measurement delays). In Fig. 4b,  $e(t)$  stays fixed in the pre-pouring phase, then decreases as the pouring proceeds (the end-effector velocity for pouring decreased accordingly). In the post-pouring phase, the robot end-effector returns to its home configuration. At the beginning of this last phase, the measurements still change due to delayed sensor outputs.

**Constrained Task and Motion Planning** – In addition to the 10 experiment trials in IV-C and IV-D, we conducted five trials to transport vessels filled with granular solids using both unconstrained and constrained motion planning techniques based on PRM\*, as well as rejection sampling (the default constrained planning method in MoveIt). Results are shown in Fig. 5. We also measured the maximum deviation from 0 across several motions using the IMU inside the Intel Realsense D435i. The maximum deviation was  $(0.026 \pm .004)$  rad for pitch and  $(0.036 \pm .004)$  rad for roll. In the experiment setup shown in Fig. 4, we measured the minimum allowed planning time needed for a valid plan to move one object to another. The constrained planner was measured to fail at a  $(37 \pm 9)\%$  greater timeout value than that of the unconstrained planner.

### C. Solubility Experiment

Solubility is the maximum amount of a substance (*solute*) that can dissolve in a specific amount of another substance (*solvent*) at a specific condition. It is a basic property of the solute and solvent, and measuring solubility is a well-known basic experiment in chemistry [33]. Solubility is measured by creating a saturated solution, a solution with the maximum concentration of solute. We measured the solubility of three solutes, table salt (sodium chloride), sugar (sucrose), and alum (aluminum potassium sulfate dodecahydrate). The workflow of the solubility experiment is shown in Fig. 6.

We evaluated the success rate of the solubility experiment by conducting several trials. An experiment is considered successful when the robot could execute all actions without aborting and could calculate solubility. An experiment is aborted when the robot arm or in-hand beaker collides with other objects, or a notable amount of water is spilled. Out of 9 experiments, 5 were successful, i.e.,  $\sim 56\%$  success rate. Note that we excluded human errors, such as misplacing glassware with respect to markers or incorrectly running software or hardware, to measure the accuracy of the proposed framework. The first mode of failure was the *inconsistency between the simulated object models and their physical counterparts*, leading to collisions during execution. Secondly, *perception errors* for object poses caused paths that were valid in simulation to collide with physical objects during execution. Lastly, the *TAMP module failed* to find a feasible plan for two experiments due to infeasible pose goal requests for constrained inverse kinematics or motion planning. We aim to improve the success rate by introducing a better perception module for more accurate simulations and developing a more robust constrained motion planner.

The results of successful solubility experiments for three solutes are shown in Table I. The primary reason for solubility error is the difficulty in visually determining whether all solutes are dissolved. The chemical solution appeared white after stirring, and the solution color prevented the inspection of white solutes inside the dish.

### D. Recrystallization Experiment

Recrystallization is a purifying technique to obtain crystals of a solute by using the difference in solubility at different temperatures. Typically, solutes have higher solubility at high temperatures, meaning hot solvents will dissolve more solute than cool solvents. The excess amount of solute that cannot be dissolved anymore while cooling the solvent precipitates

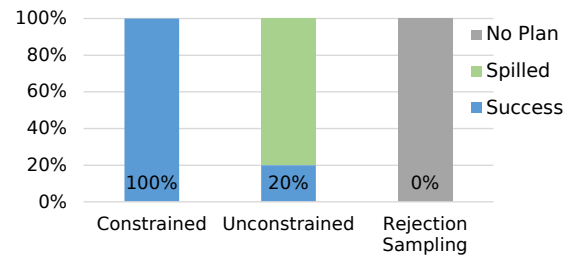


Fig. 5: Constrained planning evaluation (15 trials) against unconstrained planning and naive rejection sampling methods (5 trials each). The requested goal was to transport a vessel across the workspace, and 20 sec of planning time was allowed.

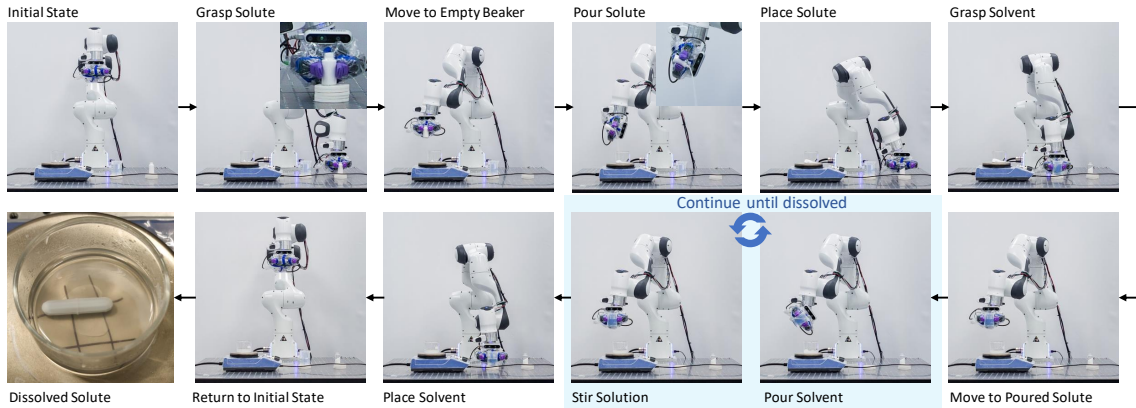


Fig. 6: **Solubility experiment of salt into the water.** First, a fixed amount of the solute is added to the dish on the weighing scale and stirrer. The robot pours a 20 g of water into the dish. A stir bar rotates by the magnetic stirrer continuously mixing the solution. After stirring, the solution is examined visually to check whether all solutes are dissolved. If solutes remain, the robot adds another 5 g of water and calculates the solubility. The experiment was conducted at room temperature (21°C).

TABLE I: **Results of the solubility experiments.** Amount of solute in the beaker, amount of water to dissolve all solute, calculated solubility (the amount of solute dissolved per 100 g of water), and literature data for solubility at 20°C is shown. Literature data are taken or calculated from [34].

<i>solute</i>	<i>solute [g]</i>	<i>water [g]</i>	<i>solubility</i>	<i>lit. data</i>	<i>% error</i>
Salt	12.96	37.51	34.6	35.8	3.62
Sugar	45.89	28.77	159.5	203.9	21.78
Alum	3.53	37.66	9.4	11.4	17.5

and forms crystals. We tested the recrystallization of alum by changing the temperature of the water. Alum was chosen as the target solute since its solubility greatly changes according to water temperature.

The recrystallization experiment setup extends the solubility test by pre-heating the solvent, i.e., the robot places the beaker with water on top of a hotplate. Then, a beaker containing alum was poured into the beaker on top of the weighing scale. The robot poured hot water into the beaker with alum. Later, the beaker was simultaneously heated by the hotplate, and the solution was stirred by the magnetic stirrer. When all the solute dissolved, the robot started to cool down the beaker by changing the temperature of the hotplate. After the solution cooled to the room temperature, we observed the formation of precipitate. Fig. 7 show the result of the experiment.



Fig. 7: **Recrystallization of alum inside the water.** Precipitation of alum was observed after cooling the solution. The dried crystals remaining at the bottom of a dish are shown.

### E. Discussion

We have shown the proposed TAMP pipeline can effectively perform constrained planning without significant additional computational cost. However, orientation constraints limit the robot’s operational workspace, and it is not possible to run constrained TAMP online. This limits how quickly the system can react and replan in a dynamic

environment, which may be problematic in the presence of humans. In terms of perception, the current use of fiducial markers inhibits the application of the proposed framework in a more realistic environment. A visual perception system that detects glassware, estimates their poses, and identifies vessel content will allow the framework to be deployed in environments without preparation [35]. The proposed pouring algorithms showed promising results, but may be limited to low-viscosity fluids and standard vessels. Hence, learning techniques for chemistry manipulation skills are an important direction for future research. Finally, the results of our experiments show the adaptability and effectiveness of our framework in performing chemistry lab automation, but system reliability is still limited. We can categorize the modes of failure mentioned in IV-C into two categories: i) failure of components, which can be resolved by enhancing their reliability or replacing their usage with alternative methods; and ii) develop new functionalities to reduce perception and environment representation inconsistencies, such as visual servoing for grasping.

### V. CONCLUSION

In this paper, we introduced a framework for automated chemical experiments using robot manipulators. The approach adapts and scales to different experiments by leveraging widely-used experiment descriptions written in XDL and existing lab tools. Through incorporating perception, constrained task and motion planning with PDDLStream, and a general skill interface, the framework can handle the dynamic workspace configurations found in existing labs. We demonstrated the capabilities of our framework through developing a system that performs three different pouring skills, executes constraint-satisfying plans, interfaces with chemistry lab hardware, and completes solubility measurement and recrystallization experiments. We aim to accelerate materials discovery by extending this framework to perform more reliable and effective experiments in the future.

## REFERENCES

- [1] C. R. Garrett, T. Lozano-Pérez, and L. P. Kaelbling, “PDDLStream: Integrating symbolic planners and blackbox samplers via optimistic adaptive planning,” in *Proceedings of the 30th International Conference on Automated Planning and Scheduling (ICAPS)*. AAAI Press, 2020, pp. 440–448.
- [2] H. Xu, Y. R. Wang, S. Eppel, A. Aspuru-Guzik, F. Shkurti, and A. Garg, “Seeing glass: Joint point-cloud and depth completion for transparent objects,” in *Annual Conference on Robot Learning*, 2021.
- [3] P. Shiri, V. Lai, T. Zepel, D. Griffin, J. Reifman, S. Clark, S. Grunert, L. P. Yunker, S. Steiner, H. Situ, *et al.*, “Automated solubility screening platform using computer vision,” *Science*, vol. 24, no. 3, p. 102176, 2021.
- [4] R. D. King, K. E. Whelan, F. M. Jones, P. G. Reiser, C. H. Bryant, S. H. Muggleton, D. B. Kell, and S. G. Oliver, “Functional genomic hypothesis generation and experimentation by a robot scientist,” *Nature*, vol. 427, no. 6971, pp. 247–252, 2004.
- [5] R. D. King, J. Rowland, S. G. Oliver, M. Young, W. Aubrey, E. Byrne, M. Liakata, M. Markham, P. Pir, L. N. Soldatova, *et al.*, “The automation of science,” *Science*, vol. 324, no. 5923, pp. 85–89, 2009.
- [6] B. Burger, P. M. Maffettone, V. V. Gusev, C. M. Aitchison, Y. Bai, X. Wang, X. Li, B. M. Alston, B. Li, R. Clowes, *et al.*, “A mobile robotic chemist,” *Nature*, vol. 583, no. 7815, pp. 237–241, 2020.
- [7] S. H. M. Mehr, M. Craven, A. I. Leonov, G. Keenan, and L. Cronin, “A universal system for digitization and automatic execution of the chemical synthesis literature,” *Science*, vol. 370, no. 6512, pp. 101–108, 2020.
- [8] H. Fakhrldeen, G. Pizzuto, J. Glowacki, and A. I. Cooper, “AR-Chemist: Autonomous robotic chemistry system architecture,” *arXiv preprint arXiv:2204.13571*, 2022.
- [9] S. Cambon, R. Alami, and F. Gravot, “A hybrid approach to intricate motion, manipulation and task planning,” *The International Journal of Robotics Research*, vol. 28, no. 1, pp. 104–126, 2009.
- [10] E. Plaku and G. D. Hager, “Sampling-based motion and symbolic action planning with geometric and differential constraints,” in *2010 IEEE International Conference on Robotics and Automation*. IEEE, 2010, pp. 5002–5008.
- [11] K. Darvish, B. Bruno, E. Simetti, F. Mastrogiorganni, and G. Casalino, “Interleaved online task planning, simulation, task allocation and motion control for flexible human-robot cooperation,” in *2018 27th IEEE International Symposium on Robot and Human Interactive Communication (RO-MAN)*, 2018, pp. 58–65.
- [12] C. R. Garrett, T. Lozano-Pérez, and L. P. Kaelbling, “FFRob: Leveraging symbolic planning for efficient task and motion planning,” *The International Journal of Robotics Research*, vol. 37, no. 1, pp. 104–136, 2018.
- [13] T. Ren, G. Chalvatzaki, and J. Peters, “Extended tree search for robot task and motion planning,” *arXiv preprint arXiv:2103.05456*, 2021.
- [14] C. Aeronautiques, A. Howe, C. Knoblock, I. D. McDermott, A. Ram, M. Veloso, D. Weld, D. W. SRI, A. Barrett, D. Christianson, *et al.*, “Pddl—the planning domain definition language,” *Technical Report, Tech. Rep.*, 1998.
- [15] M. Khodeir, B. Agro, and F. Shkurti, “Learning to search in task and motion planning with streams,” *arXiv preprint arXiv:2111.13144*, 2021.
- [16] C. R. Garrett, R. Chitnis, R. Holladay, B. Kim, T. Silver, L. P. Kaelbling, and T. Lozano-Pérez, “Integrated task and motion planning,” *Annual review of control, robotics, and autonomous systems*, vol. 4, pp. 265–293, 2021.
- [17] M. Kennedy, K. Schmeckpeper, D. Thakur, C. Jiang, V. Kumar, and K. Daniilidis, “Autonomous precision pouring from unknown containers,” *IEEE Robotics and Automation Letters*, vol. 4, no. 3, p. 2317–2324, Jul 2019.
- [18] Y. Huang, J. Wilches, and Y. Sun, “Robot gaining accurate pouring skills through self-supervised learning and generalization,” *Robotics and Autonomous Systems*, vol. 136, p. 103692, Feb 2021.
- [19] D. Berenson, S. Srinivasa, and J. Kuffner, “Task space regions: A framework for pose-constrained manipulation planning,” *The International Journal of Robotics Research*, vol. 30, no. 12, pp. 1435–1460, 2011.
- [20] B. Kim, T. T. Um, C. Suh, and F. C. Park, “Tangent bundle rrt: A randomized algorithm for constrained motion planning,” *Robotica*, vol. 34, no. 1, p. 202–225, 2016.
- [21] E. Olson, “Apriltag: A robust and flexible visual fiducial system,” in *2011 IEEE international conference on robotics and automation*. IEEE, 2011, pp. 3400–3407.
- [22] M. Helmert, “The fast downward planning system,” *Journal of Artificial Intelligence Research*, vol. 26, pp. 191–246, 2006.
- [23] Z. Kingston, M. Moll, and L. E. Kavraki, “Exploring implicit spaces for constrained sampling-based planning,” *The International Journal of Robotics Research*, vol. 38, no. 10-11, pp. 1151–1178, 2019.
- [24] P. Beeson and B. Ames, “TRAC-IK: An open-source library for improved solving of generic inverse kinematics,” in *2015 IEEE-RAS 15th International Conference on Humanoid Robots (Humanoids)*, Nov 2015, p. 928–935.
- [25] T. Yoshikawa, “Manipulability of robotic mechanisms,” *The International Journal of Robotics Research*, vol. 4, no. 2, pp. 3–9, 1985.
- [26] K. Zhang, M. Sharma, J. Liang, and O. Kroemer, “A modular robotic arm control stack for research: Franka-Interface and FrankaPy,” *arXiv preprint arXiv:2011.02398*, 2020.
- [27] I. A. Şucan, M. Moll, and L. E. Kavraki, “The Open Motion Planning Library,” *IEEE Robotics & Automation Magazine*, vol. 19, no. 4, pp. 72–82, December 2012.
- [28] D. Coleman, I. Sucan, S. Chitta, and N. Correll, “Reducing the barrier to entry of complex robotic software: a MoveIt! case study,” *arXiv preprint arXiv:1404.3785*, 2014.
- [29] JeroenDM, “elion: Constrained planning in MoveIt using OMPL’s constrained planning interface,” <https://github.com/JeroenDM/elion>, 2020.
- [30] H. R. Kam, S.-H. Lee, T. Park, and C.-H. Kim, “RViz: a toolkit for real domain data visualization,” *Telecommunication Systems*, vol. 60, no. 2, pp. 337–345, 2015.
- [31] M. Quigley, K. Conley, B. Gerkey, J. Faust, T. Foote, J. Leibs, R. Wheeler, A. Y. Ng, *et al.*, “ROS: an open-source robot operating system,” in *ICRA workshop on open source software*, vol. 3, no. 3.2. Kobe, Japan, 2009, p. 5.
- [32] NVIDIA, “Isaac Sim - robotics simulation and synthetic data generation,” <https://developer.nvidia.com/isaac-sim>, accessed on 2022-09-15.
- [33] E. Wolthuis, A. B. Pruiksma, and R. P. Heerema, “Determination of solubility: a laboratory experiment,” *Journal of Chemical Education*, vol. 37, no. 3, p. 137, 1960.
- [34] N. A. O. of Japan, *Handbook of Scientific Tables*. WORLD SCIENTIFIC, 2022.
- [35] S. Eppel, H. Xu, M. Bismuth, and A. Aspuru-Guzik, “Computer vision for recognition of materials and vessels in chemistry lab settings and the vector-labpics data set,” *ACS central science*, vol. 6, no. 10, pp. 1743–1752, 2020.